



Characterization and identification of thermoacoustic behavior of flames anchored on burner decks with multiple perforations; Transfer Function (de)composition approach

Hamed F. Ganji¹

Department of Mechanical Engineering, Eindhoven University of Technology, the Netherlands

Viktor Kornilov²

Department of Mechanical Engineering, Eindhoven University of Technology, the Netherlands

Jeroen van Oijen³

Department of Mechanical Engineering, Eindhoven University of Technology, the Netherlands

Ines Lopez Arteaga⁴

Department of Mechanical Engineering, Eindhoven University of Technology, the Netherlands
Department of Engineering Mechanics, KTH Royal Institute of Technology, Sweden

ABSTRACT

The appearance of thermoacoustic instability in combustion systems depends on thermoacoustic property (e.g., Transfer Function (TF)) of used burner/flame. Therefore, an attractive approach to cope with the instability is the purposeful design of the burner thermoacoustics. One of the ideas of how the flame TF can be altered/modified is based on the heuristic idea that the acoustic response of one flame can be counteracted by the appropriately phased response of another flame. For the particular case of premixed, burner deck anchored conical flames, the TF depends on the diameter of perforation. It suggests the concept of combining different size and shape of perforations in one burner deck. In the present work, the acoustic response of sintered ceramic fibre burners with mixed perforation is investigated using the TF (de)composition principle. By this approach, the cumulative flame TF can be represented as a weighted sum of elemental TF's of the groups of flames on the basis of the additive nature of the individual flame heat release rate. The capability of this principle to offer a designing framework for optimization of burner deck patterns aiming desirable acoustic characteristics will be tested by a course of measurements. Possible simplifications and extensions of the TF (de)composition principle will be discussed.

1. INTRODUCTION

The thermoacoustic instability arises from a closed-loop feedback between the unsteady combustion and the acoustic modes of the entire system. The acoustic wave disturbs the heat release rate of the

¹h.faghanpourganji@tue.nl

²v.kornilov@tue.nl

³j.a.v.oijen@tue.nl

⁴i.lopez@tue.nl

flame, which in turn generates acoustic fluctuations. This phenomenon not only results in loud noise, but can also cause severe physical damage to the equipment.

This is still one of the highest risks in the power generation and propulsion industry. Therefore, extensive studies have been conducted to predict and control thermoacoustic instability [1–3]. There are two ways to design this flame-acoustic wave coupling. First, one can adjust the upstream and downstream acoustics in the system-based model by using custom-built silencers/terminators [4]. Second, designing an acoustically stable combustor for the given upstream/downstream acoustics by combining different sizes and/or shapes of perforations [5]. This design approach is based on the heuristic idea that the acoustic response of one flame type can be compensated or cancelled by other flame types. These two strategies are expected to eliminate thermoacoustic instability. In the current work, However, we focus on the latter to investigate the possibility of such TF superposition.

Broadly speaking, many experimental and numerical works have been devoted to the study of the capability of flame/burner TF technique for acoustically compact flames [6–8], and even some analytical models [9–13] have been proposed. One can use these simplified mathematical expressions to identify the key parameters that affect the flame/burner dynamic response. Schuller et al. [9] obtained the acoustic response of a perturbed Bunsen-type flame due to the motion of the flame front motion caused by a uniform and convective velocity perturbation. The accuracy and validity of these models depend on the type of flow disturbance that occurs in the fresh flow. Therefore, Cuquel et al. [10] considered an incompressible divergent free convective velocity perturbation to improve the modeling of the flame front effect.

Kornilov et al. [6] studied the role of flame foot motion on flame TF. The result showed a frequency-dependent radial direction of motion of the anchoring point of the flame. Cuquel et al. [11, 14] proposed an analytical TF model of flame foot motion using the Rook model [15, 16] for the motion of planar premixed flames stabilized near the burner deck and subjected to acoustic disturbances. They included the effect of flame foot/anchor perturbations induced by an incompressible divergence-free convective velocity perturbation. The contribution of the flame foot motion in combination with the flame front motion (Bunsen-type flame) shows a saturation mechanism of the time delay at high frequency, which has been validated by a detailed measurement.

Despite significant advances in flame TF theory and identification of key parameters in thermoacoustic response of burners, its application in deliberate and systematic design has not received much attention. Kagiya [17] first proposed to select the perforation pattern such that the phase of FT for one group of holes is in antiphase to the TF phase of a second group of holes at the onset unstable frequency. Because of the mutual interaction of the flames and the difference in gain and thermal power of the grouped flames, the idea of *phase opposition* cannot be fulfilled. However, the idea of *TF compensation/cancellation* can still work through grouped flames.

Kornilov et al. [5] proposed a superposition approach to decompose the TF of multiple groups of laminar Bunsen flames. The cumulative TF was formulated for a particular composite pattern with two different circular holes and tested experimentally. The authors investigated two decomposition hypotheses: i) *same inter-flame spacing (pitch)* direct split of the composite pattern into two uniform perforation burner decks; ii) *equal open area (burner porosity)* division of the composite pattern into two uniform perforation burner decks with equal p/D , where p and D indicate pitch and diameter, respectively. A series of measurements showed that the latter resulted in better prediction. Recently, based on this principle, a local flame TF was proposed to account for spatially distributed heat release for non-acoustically compact swirling flames [18–20].

This paper takes a new look at the principle of TF(de)composition (TF(d)c) to/from individual components to experimentally test the relevance of the model for a generic burner deck patterns, which is relatively porous. Two configurations are considered to get an intuitive picture of the limitation and validity of this principle: i) mixed perforation burner deck, ii) partitioned perforation burner deck. The former are based on the second hypothesis proposed in [5], while the latter introduces the new hypothesis of using the same inter-flame spacing and burner porosity.

The rest of the article is organized as follows: Section 2.1 presents the theory of the TF(d)c principle. Then, the details of the experimental setups are described. In Section 3, the application of the TF(d)c principle is discussed using measurements on two composite burner deck configurations. Finally, in Section 4, the conclusions and an outlook on the further development of the current methodology are formulated.

2. METHODOLOGY & EXPERIMENTAL METHOD

2.1. The principle of flame TF (de)composition

A common practice to quantify the interaction of the flame with acoustic waves in the frequency domain is by the so-called flame transfer function (TF), which is defined as the ratio of the relative heat release rate perturbation (\hat{Q}'/\bar{Q}) and the relative flow perturbation (\hat{v}'/\bar{v})

$$\mathcal{F}(\omega) = \frac{\hat{Q}'}{\hat{v}'} \frac{\bar{v}}{\bar{Q}} \quad (1)$$

The fluctuations (\hat{Q}') are the result of variations of the flame surface, where undulations of the flame front are observed, while in surface burners they are caused by a fluctuating heat loss to the burner, where a pulsation of the flame at the top of the burner is observed. For premixed flames, the flame surface area is proportional to the heat release rate [21].

According to Figure 1, we first consider the general case of a composite burner deck, when the type of deck structure and flame pattern are not specified, to mathematically formulate the total flame/burner TF of a multi-flame burner from the superposition of the individual elemental patterns. According to Eq.1, the TF for both the total flame (denoted by the subscript Σ) and each individual part of the composite burner deck (index i) can be formulated as follows:

$$\mathcal{F}_{\Sigma}(\omega) = \frac{Q'_{\Sigma} \bar{v}}{\bar{Q}_{\Sigma} v'}, \quad \mathcal{F}_i(\omega) = \frac{Q'_i \bar{v}}{\bar{Q}_i v'} \quad (2)$$

Note that both the both local and global heat release rates of the TFs relate to the same upstream

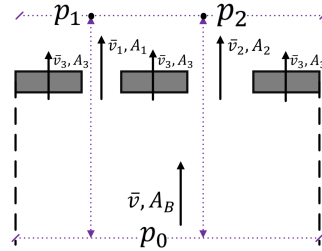


Figure 1: A sketch of flow through multiple perforations.

relative flow oscillation. One can write the total mean and acoustically perturbed parts of the flame heat release rate as follows:

$$\bar{Q}_{\Sigma} = \sum_{i=1}^{n_p} Q_i = q \sum_{i=1}^{n_p} A_i \bar{v}_i = q_v A_B \bar{v}, \quad Q'_{\Sigma} = \sum_{i=1}^{n_p} Q'_i = \sum_{i=1}^{n_p} \mathcal{F}_i(\omega) \bar{Q}_i \frac{v'}{\bar{v}} = q_v \sum_{i=1}^{n_p} \mathcal{F}_i(\omega) A_i \bar{v}_i \frac{v'}{\bar{v}} \quad (3)$$

Substitution of Eq.3 in the definition of $\mathcal{F}_{\Sigma}(\omega)$ in Eq.2 gives:

$$\mathcal{F}_{\Sigma}(\omega) = \sum_{i=1}^{n_p} \mathcal{F}_i(\omega) \frac{A_i \bar{v}_i}{A_B \bar{v}} \quad (4)$$

Eq.3 is always valid because the definition of global TF is based on the principle that energy is additive. However, using this expression requires knowledge of the local mean flow velocities \bar{v}_i and

the local TF ($\mathcal{F}_i(\omega)$) of each segment, which may depend on the surrounding flames. To overcome this difficulty, one must find a suitable manner to decompose the total flame into elementary flames. If one uses a class of composite burners with regular perforations, one can transform the Eq.3 via considering groups of individual flames. Let the subscript k enumerate these groups.

$$\mathcal{F}_\Sigma(\omega) = \sum_{k=1}^{n_k} \mathcal{F}_k(\omega) \frac{N_k A_k \bar{v}_k}{N_\Sigma A_\Sigma \bar{v}_p} \quad (5)$$

Where N_k and N_Σ are the number of flames in the group k and the total number of individual flames, A_Σ is the total area of the perforated portion of the burner deck, and $\bar{v}_p = A_B \bar{v} / A_\Sigma$ indicates the average velocity through the perforations. In practice, N_k , N_Σ , A_k , A_Σ and \bar{v} are given, so to determine the TF of the composite burner deck, the remaining task is to obtain knowledge of the local mean flow \bar{v}_k and the TF of the segmental flames $\mathcal{F}_k(\omega)$. One straightforward approach could be to introduce the concept of pressure drop measurement (PD) as shown in Fig.3, details of the setup can be found in the next section. At the same PD ($\Delta p_1 = \Delta p_2$ according to Figure 1) we can find the operating conditions for measuring the TF of a burner with uniform perforation to (de)compose the TF. Finally, Eq.5 by defining $\Omega_k = N_k A_k / \sum_{k=1}^{n_k} N_k A_k$ as the weight function of group flame k can be simplified:

$$\mathcal{F}_\Sigma(\omega) = \sum_{k=1}^{n_k} \mathcal{F}_k(\omega) \Omega_k \quad (6)$$

2.2. Apparatus

Flame/Burner TF setup

The TF technique is a common practice for measuring the response of stabilized flames to acoustic disturbances. A schematic view of the experimental setup used to measure the thermoacoustic response of premixed methane-air flames is shown in Figure 2. By definition, TF is the ratio of the relative heat release perturbation (Q'/\bar{Q}) to the upstream periodic velocity perturbations (v'/\bar{v}).

Bronkhorst Mass Flow Controllers (MFCs) are used to adjust the flow of combustible gasses. The

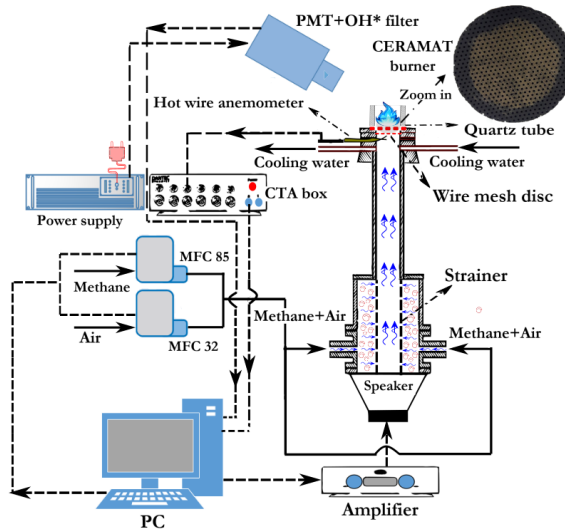


Figure 2: A schematic of Flame/Burner TF setup.

MFCs were calibrated using the setup provided by the manufacturer. Then, the amplitude of the excitation signals at frequency f with a sampling rate of $10kHz$ is adjusted to the desired range using a PC running in-house LabVIEW program. The sound generated by the computer's sound card is amplified by an amplifier and sent to the loudspeaker. To measure the periodic velocity

variations (v'), a single-sensor constant temperature anemometer (CTA) probe is placed upstream of the burner near the burner. At the same time, the flame response (heat release rate) is measured with a photomultiplier tube (PMT) equipped with a *Omega* bandpass filter designed for the OH^* radical (wavelength of $308nm$). This filter is known to be a good indicator of a premixed methane-air flame, capable of operating in the UV range as well as filtering out the possible noise of ambient light. Accordingly, the TF is rewritten in terms of the measured velocity $v_{CTA}(f)$ and the heat release rate $v_{PMT}(f)$ as follows:

$$\mathcal{F}(\omega) = \frac{\mathcal{F}(v_{PMT})}{\mathcal{F}(v_{CTA})} = \mathcal{N} \cdot G(f)e^{i\phi(f)} \quad (7)$$

Where $G(\omega)$ and $\phi(\omega)$ are the discrete frequency-dependent gain and phase of the complex $\mathcal{F}(\omega)$, respectively, \mathcal{N} and is a normalization factor to ensure that $|\mathcal{F}(\omega \rightarrow 0)| = 1$ and $\angle \mathcal{F}(\omega \rightarrow 0) = 0$, more details can be found in ([5], [22]).

Pressure drop measurement

The pressure drop (PD) across the burner surface is a key design parameter and an important performance characteristic, especially to determine the amount of flow passing through the various perforations over the burner deck. Therefore, the PD test enables us to find the required information for TF (de)composition according to section 2.2. A purpose-built equipment is shown in Figure 3a). First, a burner deck is tightly placed at the exit part of the device. Then, using a Bronkhorst MFC along with corresponding LabVIEW program, cold air (normally at $20^\circ C$) is introduced into the system. Finally, the pressure drop is measured with a fine resolution manometer. Although the measurements are carried out without combustion, it has been shown that the effect of combustion can be considered negligible [23].

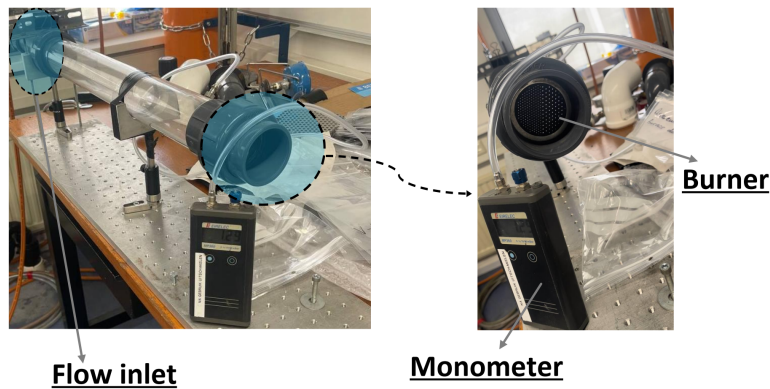


Figure 3: Pressure drop setup.

3. RESULTS DISCUSSION

The specifications of the burners in the current work are shown in the Figure 4. The total open area (burner porosity) is the same for all burners. The burner decks are $70mm$ in diameter, and the perforations/flames locate inside the disc of $50mm$ in diameter. Figure 4 a,b) show uniform perforation burners and c) mixed perforation flame holder and d) partitioned burner deck consisting of half small holes and half large holes. In the latter, we use two inter-flame spacing (pitches) corresponding to those of the uniform perforation burners. The idea is to predict the TF of composite perforated burners using TF(d)c principle by the TF of uniform perforations.

As mentioned in Section 2, to derive the formulation, one must determine the amount of mass

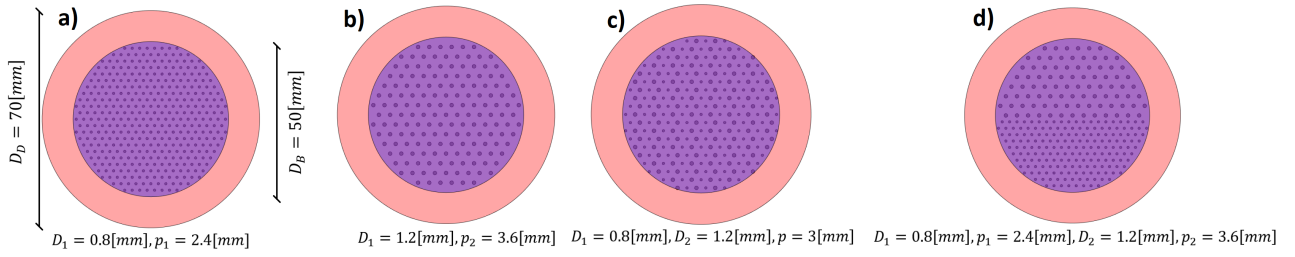


Figure 4: Burner deck configurations. a,b) Uniform perforation. c,d) Composite perforation.

flowing through different holes in order to apply the TF(d)c principle. A simple approach is to test the pressure drop (PD) of burners over a wide range of mass flow rates (see Figure 5). Then, at the operating point of interest for composite burners, one needs to read the mass flow rate on the uniformly perforated burner decks at the same PD. Following this procedure, the Table 1 and 2 are obtained for the prediction TF of the burner deck with mixed perforation and partitioned flame holder, respectively. In order to study the principle of TF(d)c comprehensively, we study this idea with low, medium and high power. The values are given in the tables can represent the full power range in an ordinary household boiler ($4kW - 25kW$) in view of the size of the sample burner here. Two different

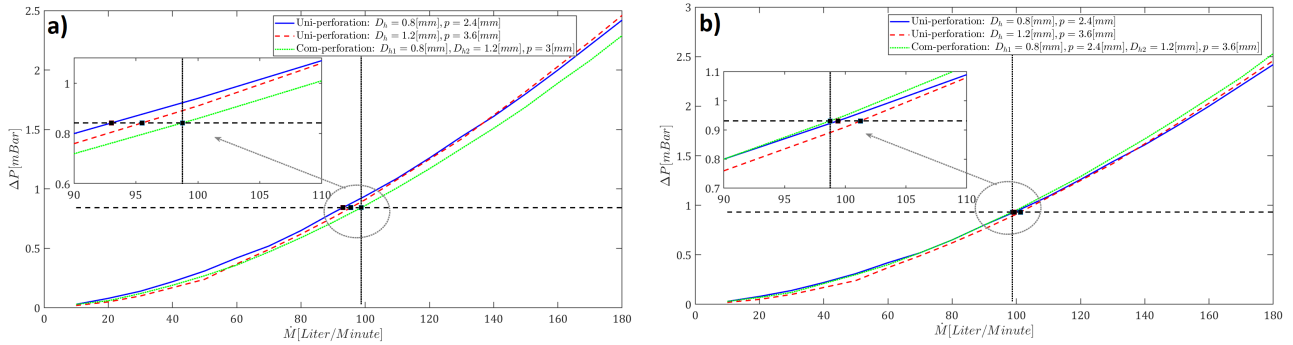


Figure 5: Pressure drop versus mass flow rate for TF (de)composition of a) mixed perforation burner deck, b) partitioned burner deck

Table 1: Operating condition (total mass flow rate $\dot{M}_t [L/min]$) at $\phi = 0.8$ for TF (de)composition of mixed perforation burner. The specification of the burners are given in Figure 4

Com-perforation	Uni-perforation 1	Uni-perforation 2
10.97	10.50	14.30
21.94	18.33	24.33
65.80	60.40	64.50

uniform burner deck configurations with $0.8mm$ and $1.2mm$ holes patterns are tested with regard to values in aforementioned tables, and the TF of composite burners (seen in Figure 4) obtained from the model are compared with direct measurement to prove the concept of TF(d)c. In this work, we use a specific Ceramic burner, which exhibits gains quite higher than usual in some operating condition. We leave the discussion about this observation for the future work.

Table 2: Operating condition (total mass flow rate $\dot{M}_t [L/min]$) at $\phi = 0.8$ for TF (de)composition of partitioned perforation burner deck. The specification of the burners are given in Figure 4

Com-perforation	Uni-perforation 1	Uni-perforation 2
10.97	10.70	14.60
21.94	19.90	25.90
65.80	65	68.30

3.1. Low thermal power

The green curve in Figure 6 represents the flame/burner TF for mixed perforation burner based on elemental burners (the blue and red curves). To prove the concept of TF(d)c, a direct TF measurement is performed on this composite sample, which is indicated with black color in the figure. The comparison with the model-based TF shows a qualitatively and quantitatively satisfactory agreement both in the gain and in the phase of the cumulative TF. In general, according to Figure 7 a), the global

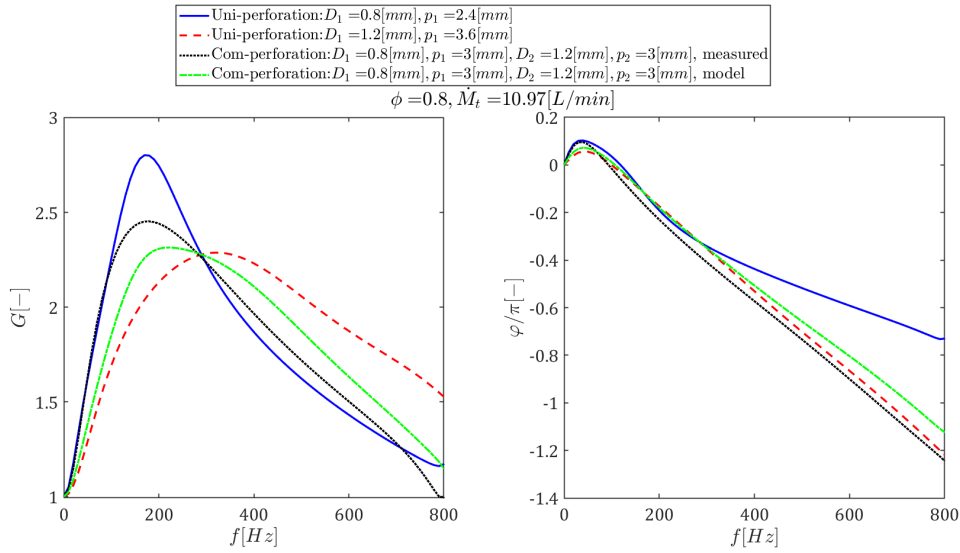


Figure 6: TF gain (right) and phase (left) for mixed perforation burner deck at low thermal power.

TF is an accumulation effect of the flame base motion (including the flat flame base and the flame foot motion) and the Bunsen/conical type flame. In the low-power cones, the half-angle decreases to $pi/2$, so that the flame looks almost flat everywhere (shown schematically in Figure b)). A slight discrepancy in the gain shown there may be due to three reasons:

- The accuracy of TF measurement is between 2–5% and the inaccuracy in determining the scale factor (calibration factor) may increase this inaccuracy.
- To determine the operating conditions, we performed the pd test following the procedure described in section 2.2. The resolution of the manometer is 0.01mbar equivalent with 1Pa. if the mass flow rate is low, as in this case, the pd value is in this range, so that may be a possible reason for this discrepancy.
- In the case of a porous burner, one usually has to decompose the TF of the porous part as well, as shown in Figure 7 with index 3. However, the PD test of the non-perforated current ceramic

burner shows very large PD. So it can be argued that a small flow pass through the burner surface. The TF measurement is not possible because the height of the flame is very small and cannot be seen even by the photomultiplier lens. Therefore, here we consider the flame on the surface indirectly by including its effect in the TF measurement of burners with base/uniform perforation. Of course, this may lead to inaccuracy in the prediction of the model basis.

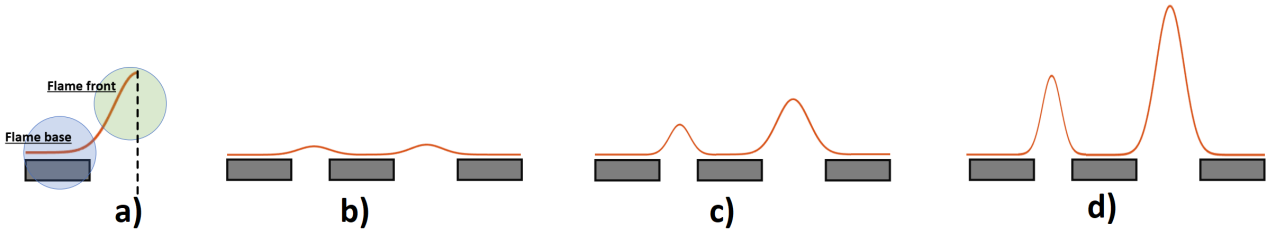


Figure 7: a) A Steady conical flame, with a focus on the flame base and the flame front region. Sketch of flame anchoring on a burner deck at , b) low thermal power, c) mid thermal power d) high thermal power.

Looking more closely at the prediction of partitioned flame holder shown in Figure 4, it can be argued that the small discrepancy in Figure 6 and 8 cannot be due to the third hypothesis above. This is because in the second composite pattern configuration corresponding to Figure 4 d), half of the burner resembles the uniform burner shown in Figure 4 a) ($D = 0.8mm, p = 2.4mm$), and the other half corresponds to the burner shown in 4 a) ($D = 1.2mm, p = 3.6mm$). Thus, the effect of the flat flame on the porous surface is globally included in the TF of the base burners. Therefore, this small discrepancy in low power could be due to the inaccuracy of the TF test and manometer resolution (first and second hypotheses above).

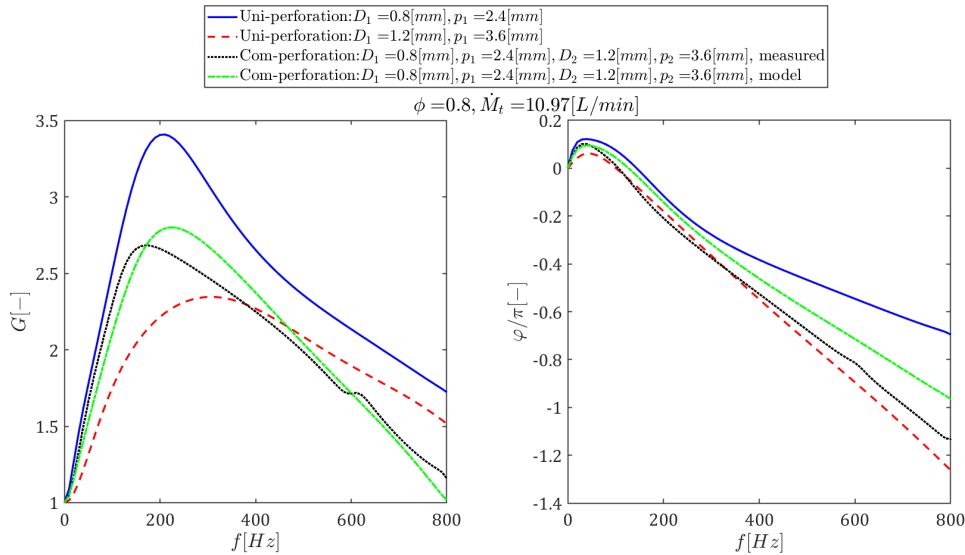


Figure 8: TF gain (right) and phase (left) for partitioned burner deck at low thermal power.

3.2. Medium thermal power

Figure 9 shows a comparison in the medium power range for mixed perforation burners. It is clear that the model does not properly evaluate the gain of the TF. This is due to the fact that, according to Figure 7 c), the collective TF is resulted from the interaction of the flat flame effect, flame foot motion, and conical flame. In order to keep the open area of a burner with mixed perforation the same as that of a uniform burner, one has to change the distance between the flames (pitch), which leads to alteration of the mutual interaction of the flame segments. There is a nonlinear coupling between the

anchoring of the flame and the perturbation of the flame front (Bunsen shape), while the phase of the model is well predicted because the phase depends strongly on the diameter of the perforation, much more than pitch.

According to Figure 10, both the gain and the phase of the cumulative TF of the partitioned burner are

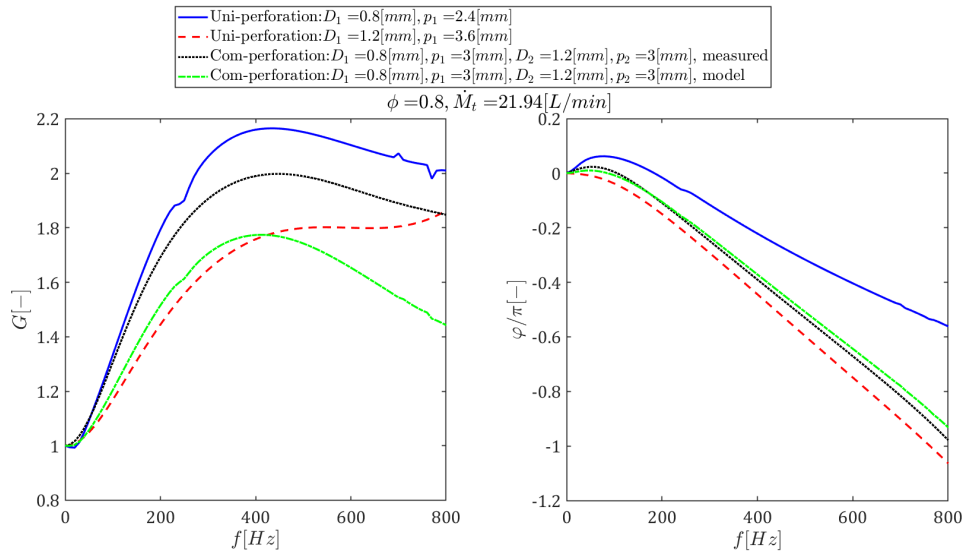


Figure 9: TF gain (right) and phase (left) for mixed perforation burner deck at mid thermal power.

in perfect qualitative and quantitative agreement with the reference value. This underlines that, given the same pitch and open area simultaneously, one can correctly account for the mutual synchronization of different flame segments.

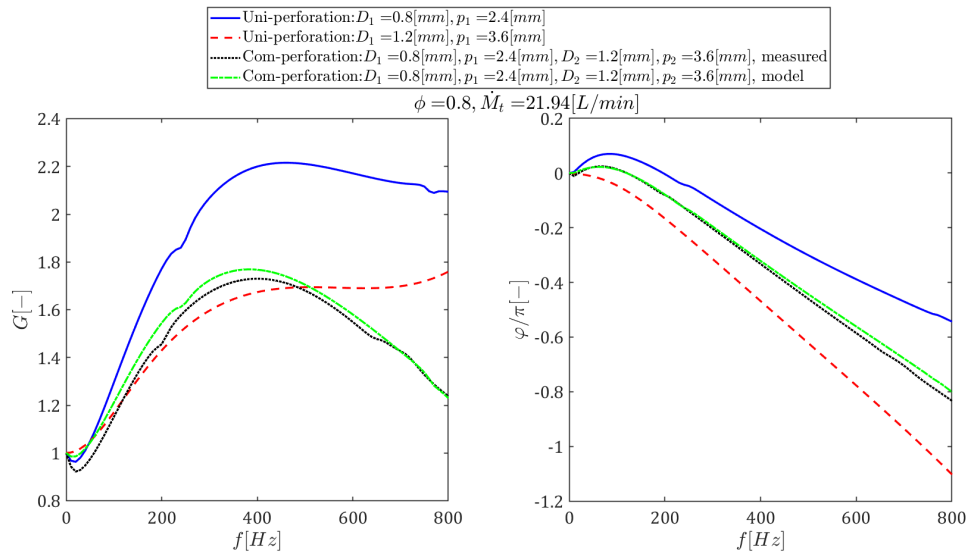


Figure 10: TF gain (right) and phase (left) for partitioned burner deck at mid thermal power.

3.3. High thermal power

At higher mass flow rates, the prediction from TF(d)c according to Figures 11 and 12 shows perfect agreement in phase and gain with the direct measurement for both the mixed perforation burner deck

and the partitioned burner. As can be seen in Figure 7 d), the effect of the conical part becomes dominant in the collective TF compared to the motion of the flame foot, so the effect of the inter-flame spacing becomes less important.

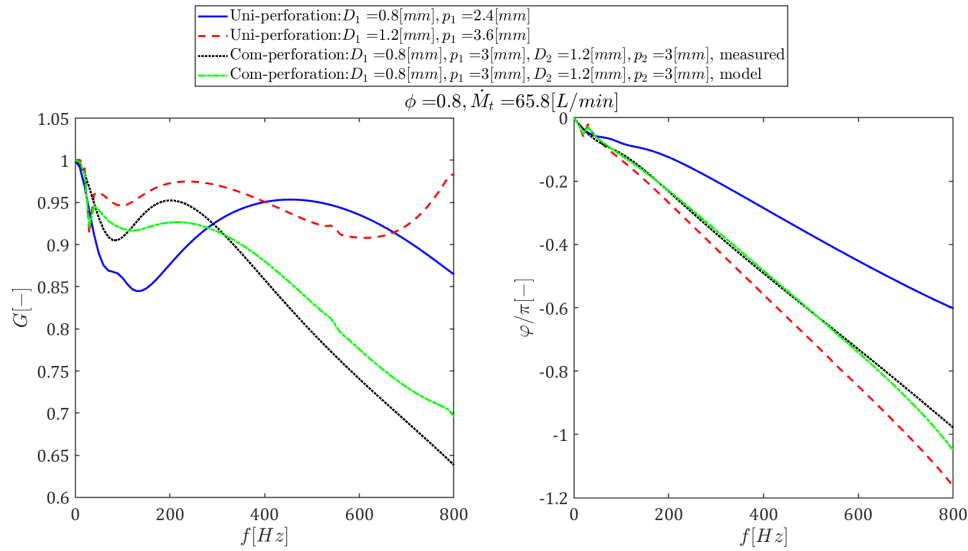


Figure 11: TF gain (right) and phase (left) for mixed perforation burner deck at high thermal power.

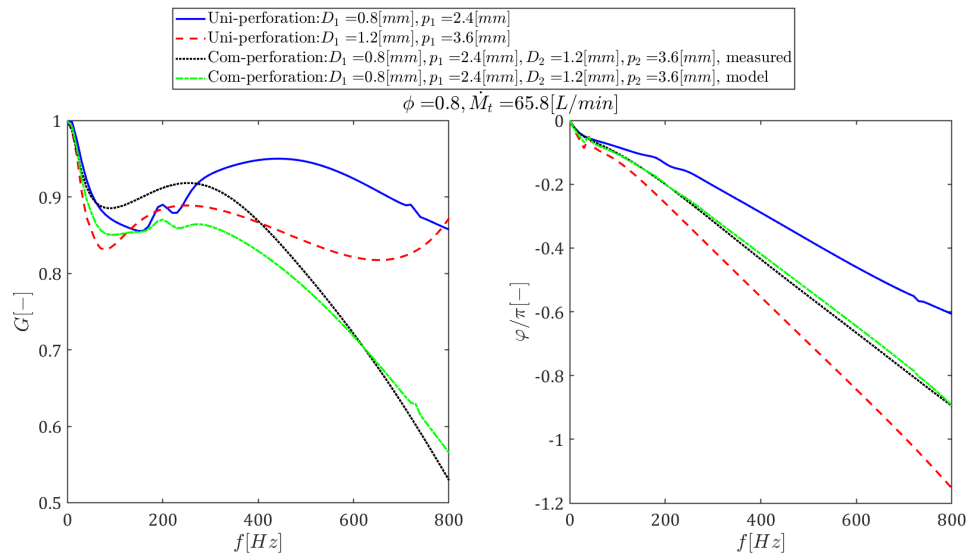


Figure 12: TF gain (right) and phase (left) for partitioned burner deck at high thermal power.

4. CONCLUSIONS

The principle of TF(d)c to/from individual components has been experimentally demonstrated for generic burner decks pattern that is relatively porous. Two configurations are considered to provide an intuitive picture of the limitation and validity of this principle: i) a mixed perforation burner deck as proposed in [5], ii) a partitioned perforation burner deck hypothesized to have equal inter-flame spacing and burner porosity. The outcome of this study can be summarized as follows:

- At low mass flow rate (thermal power): both hypotheses provide a good prediction of FT using the TF of elemental burners. A slight discrepancy can be seen, which is due to the use of pressure gauges (manometer) whose resolution is on the order of the measured PD in this operating condition, as well as the inaccuracy of the TF measurement.

- At medium power: the hypothesis of mixed perforation leads to a prediction/model that is quite far from the measurement, since in this range the global/accumulated TF interaction results from the motion of the flame base (mainly flame anchoring/foot effect) and the motion of the Bunsen-shape flame, and a change in pitch directly affects the mutual synchronization in the global ft response. By using a partitioned flame holder, one can resolve this discrepancy.
- At high power: both hypotheses provide a perfect prediction based on elementary burners' data, since the global TF is dominated by long Bunsen flames and the effect of flame base motion is negligible. Therefore, the change of pitch does not have much effect on the prediction of the mutual interaction of different perforations.

All in all, this suggests that when treating the composite TF, attention must be paid not only to the total open area (burner porosity) and the diameter similar to that of the elementary burners, but also to the distances between the flames. Therefore, it is interesting to mention that the partitioned burner concept is more predictable than the mixed perforation burner in the full thermal power range. This demonstrates the efficiency and validity of the TF(d)c principle as a tool for burner stabilization. Work is underway to take the advantage of this concept to design burner deck patterns with desirable thermoacoustic characteristics for a combustion system with given upstream and downstream terminations.

ACKNOWLEDGEMENTS

This research benefited from a full financial support from Orkli, S.Coop in Spain and the authors gratefully acknowledge it. We would also like to show our gratitude to Ignacio Sanchez and Mikel Ocana at the company who worked alongside us and provided insight, expertise and technical support that greatly assisted the research.

REFERENCES

- [1] Greg Kelsall and Christian Troger. Prediction and control of combustion instabilities in industrial gas turbines. *Applied Thermal Engineering*, 24(11-12):1571–1582, 2004.
- [2] Sébastien Candel, Daniel Durox, Thierry Schuller, Paul Palies, Jean-François Bourgouin, and Jonas P Moeck. Progress and challenges in swirling flame dynamics. *Comptes rendus mecanique*, 340(11-12):758–768, 2012.
- [3] Christian Oliver Paschereit, Ephraim Gutmark, and Wolfgang Weisenstein. Control of thermoacoustic instabilities and emissions in an industrial-type gas-turbine combustor. In *Symposium (International) on Combustion*, volume 27, pages 1817–1824. Elsevier, 1998.
- [4] Vertika Saxena, Mohammad Kojourimanesh, Viktor Kornilov, Ines Lopez Arteaga, and Philip de Goey. Designing an acoustic termination with a variable reflection coefficient to investigate the probability of instability of thermoacoustic systems. In *27th International Congress on Sound and Vibration (ICSV27)*, 2021.
- [5] VN Kornilov, M Manohar, and LPH De Goey. Thermo-acoustic behaviour of multiple flame burner decks: Transfer function (de) composition. *Proceedings of the Combustion Institute*, 32(1):1383–1390, 2009.
- [6] Viktor Nikolayevich Kornilov. Experimental research of acoustically perturbed bunsen flames, 2006.
- [7] Thierry Schuller, Sébastien Ducruix, Daniel Durox, and Sébastien Candel. Modeling tools for the prediction of premixed flame transfer functions. *Proceedings of the Combustion Institute*, 29(1):107–113, 2002.

- [8] Pierre Auzillon, Benoit Fiorina, Ronan Vicquelin, Nasser Darabiha, Olivier Gicquel, and Denis Veynante. Modeling chemical flame structure and combustion dynamics in les. *Proceedings of the Combustion Institute*, 33(1):1331–1338, 2011.
- [9] Thierry Schuller, Daniel Durox, and Sébastien Candel. A unified model for the prediction of laminar flame transfer functions: comparisons between conical and v-flame dynamics. *Combustion and flame*, 134(1-2):21–34, 2003.
- [10] A Cuquel, D Durox, and T Schuller. Theoretical and experimental determination of the flame transfer function of confined premixed conical flames. In *7th Mediterranean Combustion Symposium*, volume 36, pages 58–64. Chia Laguna, Cagliari, Sardinia, Italy, 2011.
- [11] Alexis Cuquel, Daniel Durox, and Thierry Schuller. Impact of flame base dynamics on the non-linear frequency response of conical flames. *Comptes Rendus Mécanique*, 341(1-2):171–180, 2013.
- [12] HM Altay, S Park, D Wu, D Wee, AM Annaswamy, and AF Ghoniem. Modeling the dynamic response of a laminar perforated-plate stabilized flame. *Proceedings of the Combustion Institute*, 32(1):1359–1366, 2009.
- [13] Kushal S Kedia and Ahmed F Ghoniem. An analytical model for the prediction of the dynamic response of premixed flames stabilized on a heat-conducting perforated plate. *Proceedings of the Combustion Institute*, 34(1):921–928, 2013.
- [14] Alexis Cuquel. *Dynamics and nonlinear thermo-acoustic stability analysis of premixed conical flames*. PhD thesis, Châtenay-Malabry, Ecole centrale de Paris, 2013.
- [15] R Rook, LPH De Goey, LMT Somers, KRAM Schreel, and R Parchen. Response of burner-stabilized flat flames to acoustic perturbations. *Combustion Theory and Modelling*, 6(2):223, 2002.
- [16] R Rook and LPH De Goey. The acoustic response of burner-stabilized flat flames: a two-dimensional numerical analysis. *Combustion and flame*, 133(1-2):119–132, 2003.
- [17] S Kagiya. Annual technical report digest, 10, tokyo-gaz co. *Energy and Environmental Technology Laborator*, 2000.
- [18] Kyu Tae Kim, Jong Guen Lee, BD Quay, and DA Santavicca. Spatially distributed flame transfer functions for predicting combustion dynamics in lean premixed gas turbine combustors. *Combustion and Flame*, 157(9):1718–1730, 2010.
- [19] Guoqing Wang, Thibault F Guiberti, Xi Xia, Lei Li, Xunchen Liu, William L Roberts, and Fei Qi. Decomposition of swirling flame transfer function in the complex space. *Combustion and Flame*, 228:29–41, 2021.
- [20] Guoqing Wang, Jianyi Zheng, Lei Li, Xunchen Liu, and Fei Qi. Relationship of gain and phase in the transfer function of swirling flames. *Proceedings of the Combustion Institute*, 38(4):6173–6182, 2021.
- [21] IR Hurler, RB Price, Theodore Morris Sugden, and A Thomas. Sound emission from open turbulent premixed flames. *Proceedings of the Royal Society of London. Series A. Mathematical and Physical Sciences*, 303(1475):409–427, 1968.
- [22] M Hoeijmakers. Flame-acoustic coupling in combustion instabilities [doctor thesis]. *The Netherland: Technische Universiteit Eindhoven*, 2014.
- [23] VN Kornilov, S Shakariyants, and LPH de Goey. Novel burner concept for premixed surface-stabilized combustion. In *Turbo Expo: Power for Land, Sea, and Air*, volume 44687, pages 795–801. American Society of Mechanical Engineers, 2012.